JBC Papers in Press. Published on February 25, 2013 as Manuscript M113.455105
The latest version is at http://www.jbc.org/cgi/doi/10.1074/jbc.M113.455105

Zinc deficiency impacts CO_2 assimilation and disrupts copper homeostasis in *Chlamydomonas reinhardtii**

Davin Malasarn[1], Janette Kropat[1], Scott I. Hsieh[1], Giovanni Finazzi[2,3], David Casero[4], Joseph A. Loo[1,4], Matteo Pellegrini[4,5], Francis-André Wollman[2], and Sabeeha S. Merchant[1,4*]

[1]Department of Chemistry and Biochemistry, University of California Los Angeles, Los Angeles, CA 90095

[2]CNRS, Université Paris 6, Institut de Biologie Physico-Chimique, 75005 Paris, France

[3]CNRS, Université Joseph Fourier, Commissariat à l'Energie Atomique et aux Energies Alternatives, Institut National Recherche Agronomique, UMR 5168 Laboratoire de Physiologie Cellulaire et Végétale, Institut de Recherche en Sciences et Technologie du Vivant, CEA Grenoble, 17 rue des Martyrs, 38054 Grenoble, France

[4]UCLA/DOE Institute for Genomics and Proteomics, University of California Los Angeles, Los Angeles, CA 90095

[5]Department of Molecular, Cell and Developmental Biology, University of California Los Angeles, Los Angeles, CA 90095

*Running title: Acclimation to zinc deficiency in *C. reinhardtii*

To whom correspondence should be addressed: Sabeeha S. Merchant, PhD, 607 Charles E. Young Drive East, Los Angeles, CA 90095-1569. Fax: 310-206-1035; E-mail: merchant@chem.ucla.edu

CAPSULE

Background: Zinc is required for catalysis and protein structure.
Results: Zinc deficient Chlamydomonas lose carbonic anhydrases and cannot grow photoautotrophically in air. They also hyperaccumulate copper but are phenotypically Cu-deficient and therefore require Crr1, the nutritional Cu sensor.
Conclusion: Zn-deficiency impacts the carbon concentrating mechanism and disrupts copper homeostasis.
Significance: Cross-talk between Zn and Cu homeostasis pathways.

SUMMARY

Zinc is an essential nutrient because of its role in catalysis and in protein stabilization, but excess zinc is deleterious. We distinguished four nutritional zinc states in the alga *Chlamydomonas reinhardtii*: toxic, replete, deficient and limited. Growth is inhibited in zinc-limited and zinc toxic cells relative to zinc-replete cells, while zinc-deficiency is visually asymptomatic but distinguished by the accumulation of transcripts encoding ZIP family transporters. To identify targets of zinc deficiency and mechanisms of zinc acclimation, we used RNA-seq to probe zinc nutrition responsive changes in gene expression. We identified genes encoding zinc-handling components, including ZIP family transporters and candidate chaperones. Additionally, we noted an impact on two other regulatory pathways, the carbon concentrating mechanism (CCM) and the nutritional copper regulon. Targets of transcription factor Ccm1 and various *CAH* genes are up-regulated in zinc-deficiency, likely due to reduced carbonic anhydrase activity, validated by quantitative proteomics and immunoblot analysis of Cah1, Cah3 and Cah4. Chlamydomonas is therefore not able to grow photoautotrophically in zinc-limiting conditions, but supplementation with 1% CO_2 restores growth to wild-type rates, suggesting that the inability to maintain CCM is a major consequence of zinc limitation. The Crr1 regulon responds to Cu limitation and is turned on in zinc deficiency, and Crr1 is required for growth in zinc-limiting conditions. Zinc deficient cells are functionally copper deficient, even though they hyperaccumulate copper up to 50-fold over normal levels. We suggest that zinc-deficient cells sequester Cu in a bio-unavailable form, perhaps to prevent mis-metallation of critical zinc sites.

INTRODUCTION

Zinc (Zn)[2] is an essential nutrient required in abundance by organisms ranging from bacteria to humans. Over 300 known enzymes utilize Zn as a cofactor, and whole genome surveys estimate that 4-10% of all sequenced proteins from prokaryotes and eukaryotes contain Zn-binding domains (1). Excess Zn is believed to be toxic because it can compete for metal binding sites in other proteins and can indirectly generate damaging reactive oxygen species. Thus, intracellular Zn content must be regulated to ensure that Zn-containing proteins can function while excess Zn is avoided. The first level of control is at the step of assimilation, where intracellular Zn status controls the expression and presentation of low and high affinity transporters at the plasma membrane (2-7). Another level of control is by compartmentalization, where transporters can sequester Zn in the vacuole (in fungi), lysosome-related compartments (in *C. elegans*) or in zincosomes (in mammalian cells) in a situation of excess (8-10). Sequestered Zn can be mobilized by efflux transporters (11). The expression of each type of transporter is therefore critical for homeostasis, and there are multiple levels of control from transcription to trafficking to protein degradation (2,12).

Transporters in two families are important for Zn metabolism, the ZIP family (Zrt-, Irt-like proteins), whose members function primarily to move either Zn or iron (Fe) into the cytoplasm, and the CDF (cation diffusion facilitator) family, whose members function primarily to move Zn out of the cytoplasm ((13), reviewed in (14)). In plants, members of the CDF family are also called MTPs (metal tolerance protein) because their function in moving metals out of the cytoplasm is important for handling toxicity (15,16). The pattern of expression of individual members of these families in response to the concentration and type of metal nutrient provides a clue to their physiological functions.

Photosynthetic microorganisms rely on the carbon concentrating mechanism (CCM) to

concentrate CO_2 at the active site of Rubisco, the enzyme that catalyzes the first step in the CO_2 fixation pathway (reviewed in 17,18-20). Carbonic anhydrases are integral components in this pathway and contribute to the high productivity of some of these organisms. These enzymes generally rely on a Zn cofactor (to activate water) to catalyze the interconversion of bicarbonate and CO_2. In a Zn-deficient marine environment, cobalt (Co) can replace Zn or an alternate enzyme that uses a cadmium (Cd) cofactor can substitute (21-23). The occurrence of these Zn-sparing mechanisms is indicative of the contribution of carbonic anhydrases to the cellular Zn quota, meaning the optimally desired Zn content of the cell in a Zn replete medium (24).

We have developed *Chlamydomonas reinhardtii* as a reference organism for understanding pathways of trace metal metabolism and homeostasis in algae and in the plant lineage, especially with respect to the impact of deficiency on bioenergetic pathways in the mitochondria and chloroplast (14,25). Chlamydomonas species have been found in various environmental niches distinguished by metal content, pH, and oxygen availability, suggesting that this genus has developed adaptive systems to deal with changing environmental conditions (26). In the laboratory, dilute Chlamydomonas cultures can reach stationary phase in 2 to 3 days in a simple salt-containing medium in which the trace elements are buffered by chelation with EDTA (27). The absence of serum or amino acid supplementation simplifies the provision of trace metal nutrients and the establishment of deficiency. We have been able to exploit this in previous work with Chlamydomonas cells experiencing Fe, copper (Cu), or manganese (Mn) deficiency, in which we noted that the assimilatory transporters are responsive to metal nutrition at the transcriptional level, including two genes encoding ZIP family members, which were named *IRT1* and *IRT2* because they responded to Fe-deficiency (28-31). Nevertheless, there are as many as a dozen members of the ZIP family in Chlamydomonas, and some of them are likely to be involved in Zn assimilation.

The interaction of Zn and Cu homeostasis pathways is also likely in Chlamydomonas. Cu(I) is taken up by the CTR family of transporters whose members are components of the nutritional Cu regulon in Chlamydomonas. A Zn-containing SBP-domain transcription factor named Crr1 (copper response regulator) controls the expression of the *CTR* genes (28). Its functional homolog in Arabidopsis is SPL7 (32-34). Besides the *CTR* genes encoding the plasma-membrane localized assimilatory transporters, Crr1 regulates over 60 genes involved in acclimation to Cu-deficiency through associated Cu-response elements (CuREs), which are the target sites for the SBP domain (28,35-37). The best characterized of these target genes is *CYC6* encoding cytochrome (Cyt) c_6, which is a heme-containing replacement of the usual Cu-containing protein, plastocyanin, in the photosynthetic electron transfer chain. Therefore, although Cu-deficient Chlamydomonas cells do not accumulate plastocyanin, they remain photosynthetically competent (38). Decreased plastocyanin abundance and transcriptional activation of *CYC6* are classic markers for the Cu-deficiency state.

In this work, we use growth and the expression of a subset of genes for ZIP family transporters as sentinels of Zn status to establish Zn-deficiency and Zn-limitation in Chlamydomonas, which are achieved by serial transfer of replete cells to medium lacking supplemental Zn. Transcriptome and proteome surveys identify the carbonic anhydrases and hence the carbon concentrating mechanism as a pathway impacted by poor Zn nutrition. We note also an impact on Cu homeostasis, and we suggest the existence of mechanisms that control the ratio of intracellular metal ions.

EXPERIMENTAL PROCEDURES

Culturing and strains – Chlamydomonas reinhardtii strains CC-4532 (wild-type, 2137), *crr1-2* (referred to subsequently as *crr1*), and a rescued strain *crr1-2::CRR1* (referred to subsequently as *CRR1*) was cultured under 50 – 100 µmol m^{-2} s^{-1} continuous illumination (2:1, cool white: warm white light) in Tris-Acetate-Phosphate (TAP) or Tris-Phosphate (TP) media with trace element supplements described in Kropat *et al*. (27). Briefly, stock solutions of 25 mM EDTA-Na_2, 28.5 µM $(NH_4)_6Mo_7O_{24}$, 0.1 mM Na_2SeO_3, 2.5 mM $ZnSO_4$ in 2.75 mM EDTA, 6 mM $MnCl_2$ in 6 mM EDTA, 20 mM $FeCl_3$ in 22 mM EDTA, and 2 mM $CuCl_2$ in 2 mM EDTA were made individually in Milli-Q-purified water

and diluted 1 to 1000 in the final growth medium. For metal-free studies, all glassware was triple washed in 6N hydrochloric acid followed by at least six rinses in Milli-Q purified (Millipore) water. All media were made using Milli-Q water (39). For experiments other than the proteomic studies, cells were grown in nutrient replete medium, followed by one transfer into Zn- medium with no supplemental Zn, before inoculation into the experimental conditions. For the proteomic studies, cells were grown in replete medium and directly inoculated into the experimental conditions. For experiments involving CO_2 supplementation, cultures were bubbled with filtered air (control) or a mixture of 1% CO_2 with air. Cell density was measured by counting with a haemocytometer.

Fluorescence rise and decay kinetics – For CC-4532, room temperature fluorescence rise and decay kinetics were analyzed using a FluorCam 700MF (Photon Systems Instruments). Approximately 50 µL of concentrated mid-log phase liquid culture was spotted onto the lid of a plastic petri dish and dark adapted for 10 min. prior to a flash of saturating light and measurement of the Kautsky effect in continuous red light at 150 µmol m^{-2} s^{-1} PFD with 100% actinic light and 60% activity. For measurements of *crr1* and *CRR1* cells in Zn-replete and Zn-limited conditions, room temperature kinetics were measured using a laboratory-built instrument as described in Joliot and Joliot (40).

Cell size determination – Cell size was determined with a Beckman Coulter Laser Diffraction Particle Size Analyzer LS13 320. Approximately 100 mL of cultures in exponential phase were poured into the micro liquid module with a magnetic stir bar included to keep the cells in suspension. If necessary cultures were concentrated or diluted until the sample obscuration was between 8 and 12%.

Nucleic acid analysis – Total Chlamydomonas RNA was prepared as described by Quinn and Merchant (39). RNA quality was assessed on an Agilent 2100 Bioanalyzer and by hybridization to *CBLP* (also called *RACK1*) as described previously (39). A 915-bp *Eco*RI fragment from the cDNA cloned in *pcf8-13* was used as the probe (41).

Quantitative reverse-transcriptase PCR (RT-PCR) – Genomic DNA was removed from the total RNA preparation by treatment with Turbo DNase (Ambion) according to manufacturer's instructions with the following modifications: 3 U of enzyme was used per 10 µg nucleic acid, and incubation at 37 ˚C was increased to 90 min. Complementary DNA, primed with oligo(dT), was generated with reverse transcriptase (Invitrogen) according to manufacturer's instructions. Amplification was carried out with reagents from the iQ SYBR Green Supermix qPCR kit (Bio-Rad Laboratories). Each reaction contained the vendor's master mix, 0.3 µM of each primer, and cDNA corresponding to 20 ng input RNA in the reverse transcriptase reaction. The reaction conditions for the Opticon 2 from MJ Research were: 95 ˚C for 5 min, followed by cycles of 95 ˚C for 10 s, 65 ˚C for 30 s, and 72 ˚C for 30 s, up to 40 cycles. The fluorescence was measured at each cycle at 72 ˚C and 83 ˚C. The $2^{-\Delta\Delta C}{}_T$ method was used to analyze the database on the fluorescence at 83 ˚C (42). Melting curves were performed after the PCR reaction to assess the presence of a unique final product.

RNA-seq – RNAs were sequenced by Illumina on a GAIIx system for estimating transcript abundance. The reads were aligned using Bowtie (43) in single-end mode and with a maximum tolerance of 3 mismatches to the Au10.2 transcripts sequences (http://www.phytozome.net/chlamy), corresponding to the version 4.0 assembly of the Chlamydomonas genome. Expression estimates were obtained for each individual run in units of RPKMs (reads per kilobase of mappable transcript length per million mapped reads, see (44)) after normalization by the number of aligned reads and transcript mappable length. The transcript coverage across the genome was visualized on a local installation of the UCSC browser (http://genomes.mcdb.ucla.edu/cgi-bin/hgGateway). Differential expression analysis was performed in R with the DESeq package (45) and p-values were adjusted to control for false discovery rate (FDR) with the Benjamini-Hochberg method (46). Sequence files are publicly available at NCBI's Gene Expression Omnibus, accession numbers GSE25622 and GSE41096.

Protein isolation for immunoblot analysis – Chlamydomonas cultures were collected by centrifugation (1000 ×*g*, 5 min.) and washed twice with 10 mM sodium phosphate, pH 7.0. The total

protein fraction was further subfractionated into soluble and membrane components as described in Howe and Merchant (47). Protein concentration of soluble fractions was determined using the Pierce BCA Protein Assay Kit following manufacturer's instructions. Samples were diluted to 4 µg per µL. Membrane fractions were normalized by resuspending them to a volume that was equivalent to the final soluble fraction volume.

Immunoblot analysis – Protein samples were denatured by addition of 5% ß-mercaptoethanol and boiling for 10 min before separation on denaturing polyacrylamide gels and transferring in a semi-dry blotter onto nitrocellulose membranes in transfer buffer (25 mM Tris, 192 mM glycine, 0.0004% SDS (w/v), and 20% (v/v) methanol). The membrane was blocked overnight with 1% dried milk in Tris-buffered saline (10 mM Tris-Cl, 150 mM NaCl, pH 7.5) + Tween 20 (0.05% [w/v]) before incubation in primary antiserum for 4-12 h. Gel concentrations (acrylamide monomer) and dilutions for each primary antibody were: plastocyanin, 16%, 1:1000 dilution; Cyt c_6, 16%, 1:1000 dilution; Cah1, 12%, 1:2,000 dilution; Cah3, 12%, 1:2000; Cah4, 12%, 1:15000 dilution; ferredoxin 15%, 1:10000 dilution; and CF_1, 10%, 1:20000 dilution. Secondary goat anti-rabbit horseradish peroxidase (Pierce Biotechnology) was used at a 1:5000 dilution.

Sample preparation and analysis for quantitative proteomics – Soluble protein was extracted from CC-4532 cells growing in 2.5 µM Zn and the first round of 0 supplemental Zn. For each condition, label-free, data independent quantitative liquid chromatography-tandem mass spectrometry (LC-MS/MS or "MS^E") was performed as previously described with slight modifications (35,48). In brief, cells were collected at late exponential phase from replete Zn conditions or from the first transfer to Zn-deplete medium by centrifugation. Cells were broken by slow freezing and thawing at −80 ˚C and 24 ˚C, respectively. Insoluble material was removed by centrifugation at 16,000 ×*g* for 10 minutes at 4 ˚C followed by centrifugation at 253,000 ×*g* for 20 minutes at 4 ˚C. Approximately 30 µg of protein (per lane) was separated by gel electrophoresis on 4-12% NuPage Bis-Tris gels (Invitrogen) and visualized by staining with Coomassie blue (Bio-Rad). Gel lanes were divided into ~3 mm bands and individual bands were subjected to in-gel trypsin digestion (sequencing grade modified trypsin; Promega). Digested peptides were extracted into 50/50 water/acetonitrile solution containing 2.5% formic acid and lyophilized. Peptides were then resuspended into a 25 fmol/µL of bovine serum albumin (BSA) digest and quantification standard (Waters Corporation). LC-MS^E was performed using a nanoAcquity UPLC (Waters) system coupled to a quadrupole time-of-flight mass spectrometer (Waters Xevo QTOF). Protein Lynx Global Server (PLGS version 2.4; Waters) was used to process the LC-MS raw data and determine protein identification and quantification. The quantification of protein levels was achieved via the addition of an internal protein standard (BSA trypsin digest standard) to which the data set was normalized. Our criteria were that the difference in protein abundance between growth conditions must be statistically significant ($p < 0.05$ by Student's t test) and at least 2-fold or greater in magnitude in order to define a change in protein abundance (48).

Stoichiometric measurements of cytochrome:P_{700} and PSI:PSII – Spectroscopic measurements were performed using a JTS-10 spectrophotometer (Biologic, France). Light-induced absorption changes were measured as absorption of flashed light at discrete times. Changes in the amount of functional photosynthetic complexes were evaluated measuring the electrochromic shift (ECS) spectral change, a shift in the pigment absorption bands that is linearly correlated to the number of light-induced charge separations within the reaction centers. Functional PSI and PSII content was estimated from changes in the amplitude of the fast phase of the ECS signal (at 520 nm - 546 nm) upon excitation with a saturating laser flash (520 nm, 5 ns duration). PSII contribution was calculated from the decrease in the signal amplitude upon addition of DCMU (20 µM) and hydroxylamine (2 mM) to irreversibly block PSII charge separation. Conversely, PSI was estimated as the fraction of the signal that was insensitive to these inhibitors (49). Cytochrome redox changes were calculated as the difference between the absorption at 554 nm and a baseline drawn between 545 and 573 nm and corrected for the contribution of the electrochromic signal (50). P_{700} (the primary electron donor to PSI) was measured

at 705 nm. To evaluate the relative cytochrome:P_{700} stoichiometry, measurements were performed in continuous saturating light (1100 μmol photons m^{-2} s^{-1}) and in the presence of saturating concentrations of DBMIB (10 μM). This is required to ensure full inhibition of cytochrome b_6f reduction by light generated plastoquinol, and therefore a maximum oxidation of P_{700} and of the cytochrome.

Measurement of intracellular metal content – Cells were collected by centrifugation at 1700 ×*g* for 5 min. Pellets were washed once in 1 mM EDTA to remove cell surface-associated metals and once in Milli-Q water. The washed cell paste was overlaid with nitric acid corresponding to a final concentration of 24% in 1 mL and digested at 65 ˚C. To obtain a corresponding blank, the volume of the cell paste was replaced by deionized water and treated as described above. Total metal and phosphorous content was measured by inductively coupled plasma-mass spectrometry (ICP-MS, Agilent 7500).

RESULTS

Identification of four distinct Zn nutrition states. Chlamydomonas grows in media containing a wide range of supplemental Zn concentrations (51). Elemental analysis of wild-type Chlamydomonas cells grown in standard Tris-acetate-phosphate (TAP) medium supplemented with Hutner's trace elements, which contains about 80 μM of EDTA-chelated Zn, indicated a Zn quota of approximately 2-3 × 10^7 atoms per cell. We calculated that a minimum concentration of 0.85 μM Zn ions would be necessary to support Zn-replete growth to stationary phase (~ 2 x 10^7 cells/ml). After allowing for variation in Zn quota in situations of altered physiology (e.g. low pCO_2 when carbonic anhydrases would be induced), we chose 2.5 μM Zn ions in a revised micronutrient solution (27,51,52). Indeed, this concentration of Zn is more than sufficient to support normal growth and a typical intracellular trace metal (Cu, Fe, Mn) quota; when the Zn content of the medium is reduced to 0.25 μM, there is no impact on growth (Figure 1A). Therefore, 2.5 μM Zn ions is considered metal replete for laboratory growth of Chlamydomonas.

To generate Zn limitation, we inoculated cells (to a density of 10^5 cells per ml) from a replete culture into growth medium without any Zn supplementation (labeled 0 supplemental Zn in the figures). Although all media constituents were prepared using high purity salts and all glassware was freshly acid washed (39), there remained residual Zn in the medium, which we estimated at approximately 10 nM based on ICP-MS analysis. When this culture (referred to as the 1st round in Zn-depleted medium) reached early stationary phase (~ 1 x 10^7 per ml), the cells were used to re-inoculate fresh Zn-"free" medium or medium with various amounts of supplemented Zn (Figure 1A). A growth phenotype was identified in medium supplemented with no (0) or very low (10 to 25 nM, data not shown) Zn, and this correlated with a reduced intracellular Zn content of these cultures (varying from 25% to 50% of the Zn in the replete situation in individual experiments) (Supplemental Figure S1). The Zn content of cells transferred twice to the 0 Zn medium was only slightly less than or nearly the same as that of cultures transferred once to 0 Zn medium. Further sub-culturing was therefore not necessary, and we routinely used two transfers to 0 Zn medium as the baseline for poor Zn nutrition. We also tried to generate Zn-deficiency by reducing Zn bio-availability with introduction of Zn(II)-specific chelators, like *N*, *N*, *N*', *N*'-tetrakis (2 pyridylmethyl) ethylenediamine (TPEN) into the medium, but this did not enhance the phenotype of cells in the second round of growth in 0 Zn medium. TPEN was also not effective in generating a Zn-deficient (see below) or -limitation condition when it was added at higher concentrations to Zn-replete medium. Therefore, we concluded that, in the absence of a transporter-defective mutant, sequential transfer into defined medium with 0 supplemental Zn(II) is the only effective way to generate Zn-limitation in Chlamydomonas. Analysis of the fluorescence induction curves shows that PSII activity is retained by cells growing in all concentrations of supplemental Zn, including those from cultures with no supplemental Zn, and that electron transfer between the two photosystems still operates under all of these conditions (Figure 1B). Light microscopy indicated that Zn-limited cells are larger than the replete ones, and this is confirmed by measuring the size distribution of cells in batch culture. The average diameter of Zn-limited cells is 11 μm compared to the 9 μm size of Zn-replete

cells. In addition, we noted the occurrence of smaller bodies of size ~2.5 μm in the Zn-limited culture. Their identity is not known, but they may represent stress-induced cell fragmentation (Figure 1C).

At the other extreme, Zn-excess is defined as high Zn ion concentrations at which Zn starts to become toxic and the growth rate is inhibited relative to the maximum observed growth rates. In TAP medium, growth is inhibited when the medium contains more than 125 to 250 μM chelated (EDTA) Zn ions (Figure 1A, red curve), and this defines the Zn excess situation.

In previous work on Fe nutrition, we distinguished the deficiency state from the limitation state. The Fe deficiency state is characterized by the absence of a growth phenotype or other visual symptoms, but the presence of a molecular signature, which in the case of Fe nutrition is the expression of the Fe assimilation pathway (31). Therefore, we sought to identify biomarkers for Zn-deficiency. As putative Zn transporters, members of the ZIP family are excellent candidates for Zn assimilation proteins. Previously, 14 members of this family were identified in Chlamydomonas based on homology to Arabidopsis, yeast, and human sequences (14,53). We assessed the patterns of mRNA accumulation for each of these as a function of Zn nutrition status to distinguish a) which of these might respond to Zn nutrition and b) whether their expression might be an early gauge or a sentinel of the Zn status. RNAs were isolated from cells transferred to medium containing the indicated amounts of Zn (after 1 round in 0 supplemental Zn) and analyzed by real-time RT-PCR for the expression of each of the *ZIP* genes. Among these, 5 Zn-nutrition responsive genes were identified and named *ZRT1*, *ZRT2*, *ZRT3*, *ZRT4*, and *ZRT5* for zinc-responsive transporter (Figures 2A and 2B). Based on the magnitude of the change, we chose *ZRT1* and *ZRT3* as sentinel genes and defined 25 nM as the boundary between Zn-deficiency and Zn-limiting laboratory conditions (Figure 2C).

Thus, we established growth conditions to generate each of 4 states of Zn nutrition: 0-10 nM Zn (no added Zn) for Zn-limiting conditions, 25 nM Zn for deficient conditions, 2.5 μM Zn for replete conditions, and 250 μM for Zn-toxic conditions.

Transcriptome analysis of cells growing in limited vs. replete Zn conditions. To understand the basis for growth inhibition and to discover new Zn homeostasis factors, we used RNA-Seq for an exploratory transcriptome of Zn-limited CC-4532 (wild-type) cells. The cells were generated by transfer from the first round of growth in medium with no supplemental Zn into TAP medium supplemented or not with 2.5 μM Zn-EDTA. Cells were collected from all cultures at mid-exponential phase. RNA was prepared and validated for physiology by RT-PCR for sentinel gene expression and analyzed by sequencing of cDNA libraries on the Illumina platform. The reads were aligned to the Augustus 10.2 gene models on the version 4 assembly of the Chlamydomonas genome and were analyzed to quantify abundance of transcripts as described previously. Using a cut-off of 4-fold change and a p-value of < 0.05, we identified 533 genes that showed increased transcript abundance and 119 genes that showed decreased transcript abundance in Zn-limiting conditions relative to Zn-replete conditions (Supplemental Dataset 1).

Total transcript abundance for the *ZRT* genes dramatically increased in Zn-limited conditions relative to Zn-replete conditions (Figure 3). However the proportion of each individual *ZRT* transcript in the total pool is different in the Zn-limited vs. replete state. For instance, *ZRT1* and *ZRT3* are not prominent in replete cells but become more prominent in Zn-limited conditions, suggesting that they may encode the primary high affinity assimilative Zn transporters in a situation of deficiency. ZRT5 may encode a lower affinity form that can function with higher extracellular Zn availability.

Evident in the dataset are genes belonging to 3 physiological categories: transcripts that were shown previously to increase in CO_2-limited cells (54), transcripts that increase in Cu-deficient cells (35) and transcripts encoding candidate Zn transporters and Zn homeostasis factors. The CO_2-responsive genes *HAP3* (Cre03.g177250.t1.1) and a gene encoding an unknown hypothetical protein (Cre10.g436450.t1.1) are among those whose transcripts increase most dramatically (approximately 10^3-fold), and the same is true for genes in the Cu regulon, like *CYC6* (Cre16.g651050.t1.1) encoding Cyt c_6 and a gene encoding a hypothetical protein

(Cre07.g352000.t1.1) (Table 1). The degree of regulation is as dramatic as that for the putative Zn transporters *ZRT1* (Cre07.g351950.t1.2) and *ZRT3* (Cre13.g573950.t1.2) and two genes encoding COG0523 domain-containing proteins that are implicated in Zn homeostasis (55). We named the two COG0523-domain proteins Zcp1 and Zcp2 (for Zinc-responsive COG0523 domain-containing protein). Zcp2 corresponds to Cre02.g118400.t1.2, but Zcp1 is missing in the version 4 assembly of the Chlamydomonas genome. Nevertheless, when the reads are aligned to the version 3 assembly, the increase in transcript abundance for Zcp1 (Protein ID 117458) is dramatically evident.

The Zn-responsiveness of two previously identified limiting CO_2-inducible genes prompted us to compare the genes regulated by Zn starvation to those regulated by low CO_2, including targets of the transcription factor Ccm1 (54) (Supplemental Dataset 2). We found that 82 genes were similarly Zn-responsive and CO_2-responsive, with 54 of them being predicted Ccm1 targets. Among extensively-studied low CO_2-induced genes that are also Zn-responsive are *CAH4*, *CAH5*, *CCP1*, *HLA3* and *LCIA*. When we compared the genes regulated by Zn starvation to those regulated by Cu starvation, we found a similar situation. There are 23 instances of genes responding similarly to deprivation of either micronutrient (Supplemental Dataset 3), with 16 increasing in transcript abundance and 7 decreasing, and of the 23, 11 (or about half) are Crr1 targets, which is the same fraction as that of Crr1 targets among genes that respond to Cu nutrition (35). The reason that we pick up only a fraction of the Cu regulon and Crr1 targets is because the Cu regulon is not as highly activated in Zn-deficiency as it is in Cu-deficiency and some of the transcript changes did not meet our criteria for inclusion. A few (8) genes respond in an opposite fashion to Zn vs. Cu nutrition and two of these are Crr1 targets, pointing to additional Crr1-independent controls at the transcriptional level for these two genes. When we checked the reproducibility of a subset of the changes in RNA abundance by real time RT-PCR on RNAs isolated from triplicate cultures, we confirmed the findings (data not shown).

Therefore, we conclude that a) there is a Zn nutrition-sensing regulatory pathway in Chlamydomonas that operates in part to control the abundance of transcripts for Zn transporters of the ZIP family and Zn homeostasis factors, and b) there may be an impact of Zn starvation on Cu homeostasis and CO_2 assimilation.

When we used the Algal Functional Annotation Tool (10), with selected gene ontology terms from *Arabidopsis thaliana* to overcome the limitation of available annotations for Chlamydomonas, to identify metabolic functions or pathways that might be associated with the Zn-responsive genes identified from transcriptome profiling, we noted three meaningful (p-value<0.01) biological processes for transcripts whose abundance increases: Zn and other ion transport (17 hits, scores range from 2×10^{-3} to 5×10^{-4}), Zn and other ion homeostasis (4 hits, scores range from 8×10^{-3} to 2×10^{-4}), and the response to arsenic (2 hits, score = 1×10^{-3}). For transcripts that decrease, we found genes related to organelle and peroxisome organization, organic acid metabolism, fatty acid metabolism, and regulation of cell division and DNA replication, probably a consequence of the role of Zn ions as a structural cofactor in proteins involved in nucleic acid transactions.

Proteomic analysis. To determine if changes in the transcript abundance of some genes were recapitulated at the level of the soluble proteome, we analyzed soluble protein samples by quantitative LC-MS^E from cells growing in medium supplemented with 2.5 µM Zn or in an initial round of medium with no supplemental Zn (see also (48)). We chose to use only one round of growth in medium lacking Zn in an attempt to distinguish between the primary effects of Zn deficiency vs. more general stress markers, which are likely to be more prevalent after sustained growth (i.e. two transfers) in medium with 0 supplemental Zn. Among the proteins identified as the most abundant and differentially regulated in Zn-limiting conditions are the hypothetical protein Cre07.g352000.t1.1 and both Zcp1 and Zcp2. In addition, we identified and showed an increase in the abundance of Cgl78/Ycf54 and Fea1, whose transcripts increase in both Zn-limitation and Cu-deficiency (Supplemental Dataset 3).

Carbonic anhydrases and CO_2 requirements during photoautotrophic growth. The carbon concentrating mechanism allows algae and cyanobacteria to grow phototrophically at air levels of CO_2, and carbonic anhydrases (CAs) are key enzymes in this mechanism (56-58). In

Chlamydomonas there are 12 genes predicted to encode Zn-containing carbonic anhydrases (59). The up-regulation of the CCM genes suggested to us that the activities of one or more of these enzymes might be compromised in Zn-limitation leading to a functional low CO_2 phenotype despite the presence of acetate, which normally suppresses the low CO_2-activated genes. Therefore, we surveyed the expression of the *CAH* genes that contribute to the bulk of the CA activity or that are known to be required for operation of the CCM. Cah1 is the major contributor to carbonic anhydrase activity in whole cell extracts in the presence of light and low (*i.e.* atmospheric levels) CO_2, although no phenotype has been associated with its absence. Differences in transcript accumulation for *CAH1* in response to Zn ion concentration were small but suggested a slight decrease in expression in response to decreasing Zn (Supplemental Dataset 1). Immunoblot analysis revealed a more dramatic decrease in Cah1 accumulation in Zn-limiting medium (Figure 4), and this result was recapitulated in proteomic studies (48). Cah3 is localized to the chloroplast and is believed to be the primary carbonic anhydrase required for maintenance of the CCM. Transcripts for *CAH3* increase in Zn limitation but again immunoblot analyses showed that Cah3 abundance is decreased in Zn deficiency. Two other carbonic anhydrases, Cah4 and Cah5 (nearly identical in sequence), are located in the mitochondria. The transcripts encoding these enzymes increase under Zn limitation, but immunoblot analysis revealed the decreasing abundance of Cah4 in Zn-limitation as well. We conclude that Zn limitation has a major impact on carbonic anhydrase activity, as documented already for diatoms, which led to the hypothesis that the decreased growth rate under phototrophic conditions might result from impaired CCM.

To test this hypothesis, we grew Zn-limited and Zn-replete cultures in TP medium, which lacks acetate as a carbon source, and bubbled the flasks with either air, representing limiting CO_2 conditions, or air with 1% CO_2, representing high CO_2 conditions, where CA activity is not required. In air-bubbled flasks, Zn-limited cultures displayed limited growth relative to Zn-replete cultures (Figure 5). When flasks were bubbled with 1% CO_2, growth in Zn-limited cultures was comparable to growth in Zn-replete cultures although overall growth in both cultures decreased slightly. We attribute the slight change in both cultures to a change in the pH of the medium caused by the introduction of 1% CO_2. The Zn-limitation phenotype in phototrophic medium is therefore rescued by high CO_2, establishing a causal connection between CCM and the Zn-limitation phenotype resulting from impaired CA activity. The importance of back-up CAs in diatoms for productivity in low Zn environments is evident.

Cu deficiency and Crr1 function in Zn-limited cells. The up-regulation of the Crr1 regulon and Cu-deficiency responses suggests that the Zn-deficient cells may be functionally Cu-deficient, reminiscent of the connection between Fe and Cu, where Cu-deficient cells are secondarily Fe deficient (60). To test this idea, we monitored the abundance of plastocyanin and Cyt c_6 as a function of Zn concentration by immunoblotting (Figure 4). Indeed, plastocyanin is decreased in Zn-deficient cells, and a concomitant increase in cytochrome c_6 is evident. If excess Cu is provided, we can restore plastocyanin content in proportion to the added Cu, but much greater amounts of Cu are required to maintain plastocyanin in Zn-limited cells compared to Zn-replete ones (Figure 6). This supports the idea that Zn-limited cells are functionally Cu-deficient. Therefore, we tested whether Crr1 might be required for Chlamydomonas to acclimate to Zn limitation. In Zn-limiting and toxic conditions, growth of *crr1* mutant cultures was lower than growth of the complemented strain, *CRR1* (Figure 7A). Growth of the mutant was also slightly decreased in replete conditions, consistent with the role of Crr1 in all states of Cu nutrition.

Measurement of fluorescence rise and decay kinetics in *crr1* vs. *CRR1* cells revealed that the mutant maintains a high steady state level of fluorescence emission in Zn-limitation (Figure 7B). This is likely due to the inability of the mutant to transfer electrons downstream of Photosystem II (PSII) to Photosystem I (PSI) in the photosynthetic electron transport chain, most probably as a result of the inability to upregulate Cyt c_6. To support this, we estimated the stoichiometry of Cyt c_6 to P_{700} (PSI) in Zn-limited *crr1* and *CRR1* cultures by quantifying the ratio of redox active Cyt:P_{700} using the electrochromic shift assay (Figure 7C). For the complemented

strain, Cyt:P_{700} ratios increased from 0.15 in Zn replete conditions to 0.25 in Zn-limitation, whereas the mutant showed a slight decrease in the Cyt:P_{700} ratio from 0.15 in Zn replete conditions to ~0.05 in Zn-limitation (Figure 7D). PSI:PSII ratios were approximately 1:1 for both strains in both Zn-replete and Zn-limited conditions (Figure 7D). These results support the idea that the increase in Cyt c_6 is necessary to maintain photosynthesis in Zn-limited Chlamydomonas cells, even when Cu is available in concentrations that should be sufficient to support plastocyanin maintenance.

Trace metal quota. To validate the impact of Zn nutrition on Cu content, we measured the metal content of Chlamydomonas cells over a range of supplemental Zn concentrations (Figure 8). In the range of concentrations from 25 nM to 250 µM, the Zn quota is maintained at approximately 3×10^7 atoms/cell with some variation that tracked changing external Zn concentrations. When Zn in the medium was less than 25 nM, the quota decreased to ~1×10^7 atoms/cell, consistent with symptoms of Zn deficiency and limitation. In contrast, the abundance of Fe and Cu ions (and possibly also Mn ions) increased with decreasing Zn ion supplementation. This might be attributed to up-regulation of ZIP transporters and the relatively high concentrations of these divalent cations in the medium. In fact, we note that sentinel genes for Fe assimilation are down-regulated in Zn-deficiency, presumably because of higher intracellular Fe content. Unexpectedly, given the molecular phenotype of the Cu regulon (see above), the Cu quota was increased most dramatically. Its intracellular abundance increased by over an order of magnitude from ~1-2 $\times 10^7$ atoms/cell in Zn-replete conditions to as much as 4×10^8 atoms/cell in Zn-limiting conditions. This contrasts strikingly with the tight regulation of Cu content observed in previous work (28) and presents a conundrum with respect to the molecular phenotype. We conclude that normal Cu homeostasis requires Zn.

DISCUSSION

Though studies investigating acclimation strategies to Zn deficiency have been performed in yeast and other organisms (61), the impact of Zn deficiency on photosynthetic organisms is under-investigated. Here, we have defined and characterized distinct stages of Zn nutrition in Chlamydomonas because of an excellent infrastructure for understanding trace element homeostasis developed through our prior studies (25). We have distinguished a stage where growth is inhibited and we refer to that as Zn limitation vs. a stage where the Zn-sensing signal transduction pathway is operational to turn on assimilation genes but growth is not affected, and we refer to that as deficiency. As is the case for other organisms, excess Zn results in toxicity, which is also distinguished by growth inhibition (Figure 1).

In *Saccharomyces cerevisiae* and Arabidopsis, a primary strategy for the regulation of Zn homeostasis involves the Zn-responsive expression of low and high affinity Zn transporters (62,63). Therefore, these seemed like excellent candidates for targets of nutritional Zn signaling as well. A genome survey of ZIP and CDF family transporters (14) led to the identification of 5 putative Chlamydomonas Zn transporters whose transcripts accumulate in Zn-limiting conditions (Figure 2). The regulation of these genes was used to identify Zn concentrations that induce a change in the abundance of the corresponding RNAs, and this corresponds to concentrations at which the Zn content is less than approximately 2×10^7 atoms / cell, which defines the typical Zn quota for Chlamydomonas. Very low Zn content in the medium (Zn-limitation) results in physiological stress, as suggested by the change in cell size (Figure 1) as well as by the accumulation of Nile Red-staining bodies under Zn-limiting conditions (27).

Based on fluorescence measurements of photosynthetic ability, the impact of Zn limitation did not affect the photosynthetic apparatus *per se* (Figure 1B). However, the known role of Zn in DNA-binding proteins and carbonic anhydrases (CAs) participating in the carbon concentrating mechanism (CCM) suggested that photosynthetic growth might be affected indirectly as a result of Zn deficiency. RNA-seq technology has been employed and rigorously evaluated in Chlamydomonas, showing this technology to be as quantitative as real-time PCR to evaluate changes in transcript abundance in response to external conditions (35). Therefore, we used it as an exploratory tool to discover pathways that might be impacted by poor Zn nutrition. We identified

nearly 700 genes whose expression was significantly changed in Zn limited vs. replete cells (Supplemental Dataset 1).

Photoautotrophic growth at air levels of CO_2 and carbonic anhydrases: The finding that genes described / discovered in previous studies as being targets of the CCM pathway or Crr1 pointed to inorganic carbon assimilation and Cu homeostasis, both of which affect photosynthetic performance, as being affected by poor Zn nutrition. In both cases, we substantiated this by rescuing the Zn starvation phenotype by provision of high CO_2 or excess Cu (Figures 5 and 6, respectively). Consistent with an impact on the CCM pathway, we found that photoautotrophic growth of Zn-limited cells was inhibited relative to Zn-replete cells at air levels of CO_2 (low CO_2 conditions) but provision of 1% CO_2 increased photoautotrophic growth rates in Zn-limited cells. The *LHCSR1*, *LHCSR3.1*, and *LHCSR3.2* genes encoding a sub-type of light harvesting chlorophyll binding protein are regulated by CO_2 as well, but they are inversely regulated in response to Zn limitation relative to CO_2 limitation (64). This suggests that these genes are under the control of multiple regulatory factors because they respond differently to low CO_2 than they do to other nutrient deprivation regimes, including nitrogen and sulfur starvation (65).

The most obvious targets of poor Zn nutrition are the carbonic anhydrases, and we characterized their expression profiles relative to Zn nutrition. Transcripts for some carbonic anhydrases are increased in Zn-limitation, however immunoblots for Cah1, Cah3, and Cah4/5 revealed that these proteins decreased in Zn-limiting conditions. We could not detect Cah2 because its abundance is quite low (5%) relative to that of Cah1, and indeed it is not detected in cells grown in uninduced conditons (i.e. high CO_2) (59). The discrepancy between transcript and protein accumulation may suggest post-transcriptional regulation of these genes or a compensatory upregulation of the genes in response to decreased activity. It is possible that the proteins are indeed synthesized, but they might be degraded in the absence of the essential Zn cofactor or they might be actively degraded as part of a Zn sparing program (24,48). Carbonic anhydrases are important for photosynthesis under low CO_2 conditions based on the effect of enzyme inhibitors (acetazolamide and DBS) and based on the phenotype of a mutant lacking lumenal carbonic anhydrase Cah3 (66), and the expression of several *CAH* genes is increased in cells grown at air levels of CO_2 as part of the CCM (59). The conditional CO_2-repressed phenotype of Zn-deficient Chlamydomonas cells establishes the carbonic anhydrases as key targets of Zn deficiency and therefore, in an environmental context, emphasizes the importance of the ability of diatoms to substitute Co or Cd in the active site of CAs (22,67) to maintain photosynthetic growth in face of Zn deficiency.

Influence of Zn on Cu nutrition: The similar regulation of 23 Cu-responsive genes, including 11 Crr1 targets, suggested a connection between Cu and Zn metabolism. The fraction of Crr1 targets (50%) is about the same as the fraction of the responding genes in Cu-deficient cells (35). Since most of these are genes that are highly responsive and highly expressed, we concluded that Zn-limited cells are signaling a slightly Cu-deficient status. Nevertheless, when we measured intracellular metal content, we noted the opposite – that is, several fold higher Cu content in Zn-deficient cells (Figure 8). We conclude therefore that cell-associated Cu is somehow not accessible to the Cu sensor. Further, the Cu also seems to be inaccessible to plastocyanin. The biosynthetic pathway for plastocyanin is normal because when excess Cu is added to Zn-deficient cells, this Cu can be used for holoplastocyanin synthesis and the expression of *CYC6* is decreased. Therefore, cell-associated Cu is generally not accessible for cuproprotein biosynthesis. The biosynthesis of Cyt c_6 would, in this case, become essential, which may explain the non-photosynthetic phenotype of Zn-deficient *crr1* cells (Figure 7).

The advantage, if any, of Cu-sequestration is not known. The effects of Zn nutrition on organisms is known to be complicated by the fact that interactions exist between Zn and Cu homeostasis pathways. *In vivo*, *Drosophila* metallothionein (MT) genes are induced by both Cu and Zn, suggesting that MTs bind both metals (68). Among humans, serum Cu:Zn ratios were significantly higher in patients with malignant lung tumors than in healthy patients and may serve as a diagnostic test in lung cancer patients (69). The Cu:Zn ratio is also significantly increased in

disabled elderly patients relative to healthy elderly people and was associated with levels of systemic oxidative stress (70). In the case of patients with Wilson Disease, Zn supplementation has been used to counteract Cu hyperaccumulation. Mechanistic explanations for this effect are not readily available.

Crr1 and Ccm1 are both Zn-dependent transcription factors (37,71). The maintenance of transcription factors Crr1 and Ccm1 in Zn limitation indicates that Zn remains available for their function even though carbonic anhydrase function is compromised, indicative of hierarchical rules governing the allocation of Zn ions. This mechanism has already been documented previously for Cu, Mn and Fe in Chlamydomonas (24,72). It is tempting to speculate that the COG0523 domain proteins, Zcp1 and Zcp2, may play a role in metal allocation and sparing. The corresponding genes are as highly up-regulated (~10^3-fold and ~$7x10^3$-fold, respectively) and as highly expressed (~$6x10^2$ RPKM) as are some of the genes encoding ZRT proteins (e.g. *ZRT1* and *ZRT3*). These are excellent candidates for discovery of the mechanism of regulation or the Zn sensor in Chlamydomonas. There are also a number of proteins of unknown function that are also highly regulated by Zn-deficiency, indicative of room for new discovery in Zn homeostasis.

REFERENCES

1. Andreini, C., Banci, L., Bertini, I., and Rosato, A. (2006) Zinc through the three domains of life. *J Proteome Res* **5**, 3173-3178
2. Ehrensberger, K. M., and Bird, A. J. (2011) Hammering out details: regulating metal levels in eukaryotes. *Trends Biochem Sci.* **36**, 524-531 Epub 2011 Aug 2016
3. Eide, D. J. (2009) Homeostatic and adaptive responses to zinc deficiency in *Saccharomyces cerevisiae*. *J Biol Chem.* **284**, 18565-18569 Epub 12009 Apr 18510
4. Ryu, M. S., Lichten, L. A., Liuzzi, J. P., and Cousins, R. J. (2008) Zinc transporters ZnT1 (Slc30a1), Zip8 (Slc39a8), and Zip10 (Slc39a10) in mouse red blood cells are differentially regulated during erythroid development and by dietary zinc deficiency. *J Nutr* **138**, 2076-2083
5. Dainty, S. J., Kennedy, C. A., Watt, S., Bahler, J., and Whitehall, S. K. (2008) Response of Schizosaccharomyces pombe to zinc deficiency. *Eukaryot Cell* **7**, 454-464
6. Zhao, H., and Eide, D. (1996) The *ZRT2* gene encodes the low affinity zinc transporter in *Saccharomyces cerevisiae*. *J Biol Chem* **271**, 23203-23210
7. Zhao, H., and Eide, D. (1996) The yeast *ZRT1* gene encodes the zinc transporter protein of a high-affinity uptake system induced by zinc limitation. *Proc Natl Acad Sci U S A* **93**, 2454-2458
8. Simm, C., Lahner, B., Salt, D., LeFurgey, A., Ingram, P., Yandell, B., and Eide, D. J. (2007) *Saccharomyces cerevisiae* vacuole in zinc storage and intracellular zinc distribution. *Eukaryot Cell.* **6**, 1166-1177 Epub 2007 May 1125
9. Roh, H. C., Collier, S., Guthrie, J., Robertson, J. D., and Kornfeld, K. (2012) Lysosome-related organelles in intestinal cells are a zinc storage site in *C. elegans*. *Cell Metab* **15**, 88-99
10. Ballestin, R., Molowny, A., Marin, M. P., Esteban-Pretel, G., Romero, A. M., Lopez-Garcia, C., Renau-Piqueras, J., and Ponsoda, X. (2011) Ethanol reduces zincosome formation in cultured astrocytes. *Alcohol Alcohol.* **46**, 17-25 Epub 2010 Dec 2011
11. Williams, L. E., Pittman, J. K., and Hall, J. L. (2000) Emerging mechanisms for heavy metal transport in plants. *Biochim Biophys Acta* **1465**, 104-126
12. Kambe, T., and Andrews, G. K. (2009) Novel proteolytic processing of the ectodomain of the zinc transporter ZIP4 (SLC39A4) during zinc deficiency is inhibited by acrodermatitis enteropathica mutations. *Mol Cell Biol* **29**, 129-139
13. Davis, D. E., Roh, H. C., Deshmukh, K., Bruinsma, J. J., Schneider, D. L., Guthrie, J., Robertson, J. D., and Kornfeld, K. (2009) The cation diffusion facilitator gene cdf-2 mediates zinc metabolism in *Caenorhabditis elegans*. *Genetics* **182**, 1015-1033
14. Blaby-Haas, C. E., and Merchant, S. S. (2012) The ins and outs of algal metal transport. *Biochim Biophys Acta* **1823**, 1531-1552
15. Kim, D., Gustin, J. L., Lahner, B., Persans, M. W., Baek, D., Yun, D. J., and Salt, D. E. (2004) The plant CDF family member TgMTP1 from the Ni/Zn hyperaccumulator *Thlaspi goesingense* acts to enhance efflux of Zn at the plasma membrane when expressed in *Saccharomyces cerevisiae*. *Plant J* **39**, 237-251
16. Podar, D., Scherer, J., Noordally, Z., Herzyk, P., Nies, D., and Sanders, D. (2012) Metal selectivity determinants in a family of transition metal transporters. *J Biol Chem* **287**, 3185-3196
17. Badger, M. R., and Price, G. D. (2003) CO_2 concentrating mechanisms in cyanobacteria: molecular components, their diversity and evolution. *J Exp Bot.* **54**, 609-622
18. Giordano, M., Beardall, J., and Raven, J. A. (2005) CO_2 concentrating mechanisms in algae: mechanisms, environmental modulation, and evolution. *Annu Rev Plant Biol.* **56**, 99-131
19. Roberts, K., Granum, E., Leegood, R. C., and Raven, J. A. (2007) Carbon acquisition by diatoms. *Photosynth Res.* **93**, 79-88 Epub 2007 May 2012
20. Wang, Y., Duanmu, D., and Spalding, M. H. (2011) Carbon dioxide concentrating mechanism in *Chlamydomonas reinhardtii*: inorganic carbon transport and CO_2 recapture. *Photosynth Res.* **109**, 115-122 Epub 2011 Mar 2016
21. Lane, T. W., and Morel, F. M. (2000) A biological function for cadmium in marine diatoms. *Proc Natl Acad Sci U S A.* **97**, 4627-4631

22. Lane, T. W., and Morel, F. M. (2000) Regulation of carbonic anhydrase expression by zinc, cobalt, and carbon dioxide in the marine diatom *Thalassiosira weissflogii*. *Plant Physiol.* **123**, 345-352
23. Yee, D., and Morel, F. M. M. (1996) In vivo substitution of zinc by cobalt in carbonic anhydrase of a marine diatom. *Limnol Oceanogr* **41**, 573-577
24. Merchant, S. S., and Helmann, J. D. (2012) Elemental economy: microbial strategies for optimizing growth in the face of nutrient limitation. *Adv Microb Physiol* **60**, 91-210
25. Merchant, S. S., Allen, M. D., Kropat, J., Moseley, J. L., Long, J. C., Tottey, S., and Terauchi, A. M. (2006) Between a rock and a hard place: Trace element nutrition in Chlamydomonas. *Biochim Biophys Acta.* **1763**, 578-594 Epub 2006 Apr 2026
26. Harris, E. H. (1989) *The Chlamydomonas Sourcebook: A comprehensive guide to biology and laboratory use*, Academic Press, San Diego, CA
27. Kropat, J., Hong-Hermesdorf, A., Casero, D., Ent, P., Castruita, M., Pellegrini, M., Merchant, S. S., and Malasarn, D. (2011) A revised mineral nutrient supplement increases biomass and growth rate in *Chlamydomonas reinhardtii*. *Plant J* **66**, 770-780 doi: 710 1111/j 1365-1313X 2011 04537 x Epub 02011 Mar 04521
28. Page, M. D., Kropat, J., Hamel, P. P., and Merchant, S. S. (2009) Two *Chlamydomonas* CTR copper transporters with a novel cys-met motif are localized to the plasma membrane and function in copper assimilation. *Plant Cell.* **21**, 928-943 Epub 2009 Mar 2024 PMC2671701
29. Allen, M. D., del Campo, J. A., Kropat, J., and Merchant, S. S. (2007) *FEA1*, *FEA2*, and *FRE1*, encoding two homologous secreted proteins and a candidate ferrireductase, are expressed coordinately with *FOX1* and *FTR1* in iron-deficient *Chlamydomonas reinhardtii*. *Eukaryot Cell.* **6**, 1841-1852 Epub 2007 Jul 1827 PMC2043389
30. Allen, M. D., Kropat, J., Tottey, S., Del Campo, J. A., and Merchant, S. S. (2007) Manganese deficiency in Chlamydomonas results in loss of photosystem II and MnSOD function, sensitivity to peroxides, and secondary phosphorus and iron deficiency. *Plant Physiol.* **143**, 263-277 Epub 2006 Nov 2003 PMC1761973
31. La Fontaine, S., Quinn, J. M., Nakamoto, S. S., Page, M. D., Göhre, V., Moseley, J. L., Kropat, J., and Merchant, S. (2002) Copper-dependent iron assimilation pathway in the model photosynthetic eukaryote *Chlamydomonas reinhardtii*. *Eukaryot Cell* **1**, 736-757
32. Kropat, J., Tottey, S., Birkenbihl, R. P., Depège, N., Huijser, P., and Merchant, S. (2005) A regulator of nutritional copper signaling in *Chlamydomonas* is an SBP domain protein that recognizes the GTAC core of copper response element. *Proc Natl Acad Sci U S A.* **102**, 18730-18735 Epub 12005 Dec 18713 PMC1311908
33. Yamasaki, H., Hayashi, M., Fukazawa, M., Kobayashi, Y., and Shikanai, T. (2009) *SQUAMOSA* Promoter Binding Protein-Like7 Is a Central Regulator for Copper Homeostasis in *Arabidopsis*. *Plant Cell.* **21**, 347-361 Epub 2009 Jan 2002
34. Bernal, M., Casero, D., Singh, V., Wilson, G. T., Grande, A., Yang, H., Dodani, S. C., Pellegrini, M., Huijser, P., Connolly, E. L., Merchant, S. S., and Kramer, U. (2012) Transcriptome sequencing identifies SPL7-regulated copper acquisition genes FRO4/FRO5 and the copper dependence of iron homeostasis in Arabidopsis. *Plant Cell* **24**, 738-761
35. Castruita, M., Casero, D., Karpowicz, S. J., Kropat, J., Vieler, A., Hsieh, S. I., Yan, W., Cokus, S., Loo, J. A., Benning, C., Pellegrini, M., and Merchant, S. S. (2011) Systems biology approach in Chlamydomonas reveals connections between copper nutrition and multiple metabolic steps. *Plant Cell.* **23**, 1273-1292 Epub 2011 Apr 1215
36. Quinn, J. M., Barraco, P., Eriksson, M., and Merchant, S. (2000) Coordinate copper- and oxygen-responsive *Cyc6* and *Cpx1* expression in *Chlamydomonas* is mediated by the same element. *J Biol Chem* **275**, 6080-6089
37. Sommer, F., Kropat, J., Malasarn, D., Grossoehme, N. E., Chen, X., Giedroc, D. P., and Merchant, S. S. (2010) The CRR1 nutritional copper sensor in *Chlamydomonas* contains two distinct metal-responsive domains. *Plant Cell.* **22**, 4098-4113 Epub 2010 Dec 4093

38. Merchant, S., and Bogorad, L. (1986) Regulation by copper of the expression of plastocyanin and cytochrome c_{552} in *Chlamydomonas reinhardtii*. *Mol Cell Biol* **6**, 462-469
39. Quinn, J. M., and Merchant, S. (1998) Copper-responsive gene expression during adaptation to copper deficiency. *Methods Enzymol* **297**, 263-279
40. Joliot, P., and Joliot, A. (2002) Cyclic electron transfer in plant leaf. *Proc Natl Acad Sci U S A* **99**, 10209-10214
41. Schloss, J. A. (1990) A *Chlamydomonas* gene encodes a G protein beta subunit-like polypeptide. *Mol Gen Genet* **221**, 443-452
42. Livak, K. J., and Schmittgen, T. D. (2001) Analysis of relative gene expression data using real-time quantitative PCR and the $2^{-\Delta\Delta C}_{T}$ Method. *Methods* **25**, 402-408
43. Langmead, B., Trapnell, C., Pop, M., and Salzberg, S. L. (2009) Ultrafast and memory-efficient alignment of short DNA sequences to the human genome. *Genome Biol* **10**, R25
44. Mortazavi, A., Williams, B. A., McCue, K., Schaeffer, L., and Wold, B. (2008) Mapping and quantifying mammalian transcriptomes by RNA-Seq. *Nat Methods.* **5**, 621-628 Epub 2008 May 2030
45. Anders, S., and Huber, W. (2010) Differential expression analysis for sequence count data. *Genome Biol* **11**, R106
46. Benjamini, Y., and Hochberg, Y. (1995) Controlling the False Discovery Rate: A Practical and Powerful Approach to Multiple Testing. *Journal of the Royal Statistical Society. Series B (Methodological)* **57**, 289-300
47. Howe, G., and Merchant, S. (1992) The biosynthesis of membrane and soluble plastidic c-type cytochromes of *Chlamydomonas reinhardtii* is dependent on multiple common gene products. *Embo J* **11**, 2789-2801
48. Hsieh, S. I., Castruita, M., Malasarn, D., Urzica, E., Erde, J., Page, M. D., Yamasaki, H., Casero, D., Pellegrini, M., Merchant, S. S., and Loo, J. A. (2013) The Proteome of Copper, Iron, Zinc, and Manganese Micronutrient Deficiency in *Chlamydomonas reinhardtii*. *Mol Cell Proteomics*12, 65-86
49. Bailleul, B., Cardol, P., Breyton, C., and Finazzi, G. (2010) Electrochromism: a useful probe to study algal photosynthesis. *Photosynth Res* **106**, 179-189
50. Finazzi, G., Buschlen, S., de Vitry, C., Rappaport, F., Joliot, P., and Wollman, F. A. (1997) Function-directed mutagenesis of the cytochrome b_6f complex in *Chlamydomonas reinhardtii*: involvement of the cd loop of cytochrome b_6 in quinol binding to the Q_o site. *Biochemistry* **36**, 2867-2874
51. Harris, E. H. (2009) *Introduction to Chlamydomonas and Its Laboratory Use*, Elsevier, San Diego, CA
52. Hutner, S. H., Provasoli, L., Schatz, A., and Haskins, C. P. (1950) Some approaches to the study of the role of metals in the metabolism of microorganisms. *Proc. Amer. Philosophical Soc.* **94**, 152-170
53. Hanikenne, M., Krämer, U., Demoulin, V., and Baurain, D. (2005) A comparative inventory of metal transporters in the green alga *Chlamydomonas reinhardtii* and the red alga *Cyanidioschizon merolae*. *Plant Physiol* **137**, 428-446
54. Fang, W., Si, Y., Douglass, S., Casero, D., Merchant, S. S., Pellegrini, M., Ladunga, I., Liu, P., and Spalding, M. H. (2012) Transcriptome-wide changes in *Chlamydomonas reinhardtii* gene expression regulated by carbon dioxide and the CO_2-concentrating mechanism regulator CIA5/CCM1. *Plant Cell* **24**, 1876-1893
55. Haas, C. E., Rodionov, D. A., Kropat, J., Malasarn, D., Merchant, S. S., and de Crécy-Lagard, V. (2009) A subset of the diverse COG0523 family of putative metal chaperones is linked to zinc homeostasis in all kingdoms of life. *BMC Genomics.* **10**, 470 PMC2770081
56. Tachiki, A., Fukuzawa, H., and Miyachi, S. (1992) Characterization of carbonic anhydrase isozyme CA2, which is the CAH2 gene product, in Chlamydomonas reinhardtii. *Biosci Biotechnol Biochem* **56**, 794-798

57. Villarejo, A., Rolland, N., Martinez, F., and Sültemeyer, D. (2001) A new chloroplast envelope carbonic anhydrase activity is induced during acclimation to low inorganic carbon concentrations in *Chlamydomonas reinhardtii*. *Planta* **213**, 286-295
58. Ynalvez, R. A., Xiao, Y., Ward, A. S., Cunnusamy, K., and Moroney, J. V. (2008) Identification and characterization of two closely related β-carbonic anhydrases from *Chlamydomonas reinhardtii*. *Physiol Plant.* **133**, 15-26
59. Moroney, J. V., Ma, Y., Frey, W. D., Fusilier, K. A., Pham, T. T., Simms, T. A., DiMario, R. J., Yang, J., and Mukherjee, B. (2011) The carbonic anhydrase isoforms of *Chlamydomonas reinhardtii*: intracellular location, expression, and physiological roles. *Photosynth Res.* **109**, 133-149 Epub 2011 Mar 2012
60. Dancis, A., Haile, D., Yuan, D. S., and Klausner, R. D. (1994) The *Saccharomyces cerevisiae* copper transport protein (Ctr1p). Biochemical characterization, regulation by copper, and physiologic role in copper uptake. *J Biol Chem* **269**, 25660-25667
61. Rutherford, J. C., and Bird, A. J. (2004) Metal-responsive transcription factors that regulate iron, zinc, and copper homeostasis in eukaryotic cells. *Eukaryot Cell* **3**, 1-13
62. Eide, D. J. (2006) Zinc transporters and the cellular trafficking of zinc. *Biochim Biophys Acta* **1763**, 711-722
63. Sinclair, S. A., and Kramer, U. (2012) The zinc homeostasis network of land plants. *Biochim Biophys Acta* **1823**, 1553-1567
64. Yamano, T., Miura, K., and Fukuzawa, H. (2008) Expression analysis of genes associated with the induction of the carbon-concentrating mechanism in *Chlamydomonas reinhardtii*. *Plant Physiol* **147**, 340-354
65. Toepel, J., Albaum, S. P., Arvidsson, S., Goesmann, A., la Russa, M., Rogge, K., and Kruse, O. (2011) Construction and evaluation of a whole genome microarray of *Chlamydomonas reinhardtii*. *BMC Genomics* **12**, 579
66. Sinetova, M. A., Kupriyanova, E. V., Markelova, A. G., Allakhverdiev, S. I., and Pronina, N. A. (2012) Identification and functional role of the carbonic anhydrase Cah3 in thylakoid membranes of pyrenoid of *Chlamydomonas reinhardtii*. *Biochim Biophys Acta* **1817**, 1248-1255
67. Lane, T. W., Saito, M. A., George, G. N., Pickering, I. J., Prince, R. C., and Morel, F. M. (2005) Biochemistry: a cadmium enzyme from a marine diatom. *Nature* **435**, 42
68. Zhang, B., Egli, D., Georgiev, O., and Schaffner, W. (2001) The *Drosophila* homolog of mammalian zinc finger factor MTF-1 activates transcription in response to heavy metals. *Mol Cell Biol* **21**, 4505-4514
69. Diez, M., Cerdan, F. J., Arroyo, M., and Balibrea, J. L. (1989) Use of the copper/zinc ratio in the diagnosis of lung cancer. *Cancer* **63**, 726-730
70. Mezzetti, A., Pierdomenico, S. D., Costantini, F., Romano, F., De Cesare, D., Cuccurullo, F., Imbastaro, T., Riario-Sforza, G., Di Giacomo, F., Zuliani, G., and Fellin, R. (1998) Copper/zinc ratio and systemic oxidant load: effect of aging and aging-related degenerative diseases. *Free Radic Biol Med* **25**, 676-681
71. Fukuzawa, H., Miura, K., Ishizaki, K., Kucho, K. I., Saito, T., Kohinata, T., and Ohyama, K. (2001) Ccm1, a regulatory gene controlling the induction of a carbon-concentrating mechanism in *Chlamydomonas reinhardtii* by sensing CO_2 availability. *Proc Natl Acad Sci USA*. **98**, 5347-5352 Epub 2001 Apr 5343
72. Page, M. D., Allen, M. D., Kropat, J., Urzica, E. I., Karpowicz, S. J., Hsieh, S. I., Loo, J. A., and Merchant, S. S. (2012) Fe sparing and Fe recycling contribute to increased superoxide dismutase capacity in iron-starved *Chlamydomonas reinhardtii*. *Plant Cell* **24**, 2649-2665

Acknowledgments—We thank Rey Martin, Kara Velez and Esperanza del Rio for their assistance during the early phases of the project, Joan Valentine at UCLA for use of the ICP-MS for metal measurements, Dr. James V. Moroney for providing antibodies to Cah1 and Cah4, Dr. Martin Spalding for providing an additional antibody for Cah1, and Dr. Joanna Porankiewicz for providing an antibody to Cah3.

Footnotes

*The work on the zinc-deficiency transcriptome was supported by the National Institutes of Health (NIH) (GM42143 to SM). The proteomic analyses and expression of proteins for use as antigens were supported by Institute of Genomics and Proteomics at UCLA (funded by the Office of Science (BER), U.S. Department of Energy through Cooperative Agreement No. DE-FC02-02ER63421). SIH was supported in part by a Ruth L. Kirschstein National Research Service Award from the NIH (T32 GM07185) for UCLA's predoctoral Cellular and Molecular Biology Training Program. DM was supported in part by an NIH Ruth L. Kirschstein National Research Service Award (F32GM083562) and a Chateaubriand Fellowship for collaborative experiments with GF and FAW.

[1]To whom correspondence may be addressed: 607 Charles E. Young Drive East, Los Angeles, CA 90095-1569. Fax: 310-206-1035; E-mail: merchant@chem.ucla.edu

[2] The elemental abbreviations will be used throughout the article without indication of speciation, ionic or oxidation state, unless relevant.

FIGURE LEGENDS

FIGURE 1. Phenotypes of Zn-deficient Chlamydomonas. Strain CC-4532 was grown in TAP medium with different amounts of supplemental Zn (in μM): 0 (black), 0.25 (blue), 2.5 (green), 80 (purple), and 250 (red). (A) Growth measured by counting cells, (B) Kautsky fluorescence rise and decay kinetics, (C) diameters of cells growing in medium containing 2.5 μM Zn (left) and 0 supplemental Zn (right). Growth curves represent the averages of biological triplicates from three separate inocula (s.d. not shown for clarity). For fluorescence measurements and cell size determination, representative data from experimental triplicates are shown.

FIGURE 2. Relative expression of ZIP family transporter genes identifies a subset responsive to Zn nutrition. RNA was isolated from cells grown in TAP medium containing various amounts of Zn or Cu supplementation as described below. RNA abundance was assessed by real-time RT-PCR using the $2^{-\Delta\Delta C_T}$ method. RNA abundance was normalized to *CBLP* abundance, and average C_T values were calculated from technical triplicates. Each data point represents an independent RNA sample. (A) RNA abundance in 0 Zn relative to 2.5 μM Zn supplementation. (B) RNA abundance in 0 Cu relative to 2 μM Cu supplementation. (C) *ZRT1* (left) and *ZRT3* (right) mRNA abundances in cells grown in medium containing 0, 0.025, 0.25, 2.5, 25, 80, 125, and 250 μM supplemental Zn. The Zn deficient state was identified as the concentration of supplemental Zn at which *ZRT1* (left) and *ZRT3* (right) transcripts increased relative to 2.5 μM Zn supplementation (replete conditions).

FIGURE 3. Abundance of Chlamydomonas *ZRT* transcripts. Pie charts show the contribution of each *ZRT* transcript during growth in Zn-limited (no supplemental Zn) and Zn-replete (2.5 μM Zn) media. The size of each pie chart represents the sum of all *ZRT* transcripts in that condition relative to the other.

FIGURE 4. Impact of Zn nutrition on abundance of select proteins in the photosynthetic apparatus. Total soluble and resuspended particulate fractions from Chlamydomonas cultures grown in TAP medium with the various supplemental Zn concentrations were separated on polyacrylamide gels under denaturing conditions. Lanes: 1 = 0 Zn, 2 = 0.25 μM Zn, 3 = 2.5 μM Zn, 4 = 25 μM Zn, 5 = 80 μM Zn, 6 = 125 μM Zn. The separated proteins were transferred to nitrocellulose membranes. Proteins of interest were detected by immunoblot analysis with antisera raised against cytochrome c_6 (Cyt c_6), plastocyanin (PC), carbonic anhydrase 1 (CAH1), carbonic anhydrase 3 (CAH3), carbonic anhydrase 4 (CAH4), ferredoxin (FD), and the alpha and beta subunits of the chloroplast ATP synthase (α/ß CF_1). For Cyt c_6 and α/ß CF_1, dilutions of max. are based on lane 1. For all other proteins, dilutions of max. are based on lane 6.

FIGURE 5. High CO_2 suppresses the growth phenotype of Zn-limited photoautotrophically grown cells. Chlamydomonas cells (strain CC-4532) were pre-conditioned in TP medium and inoculated to a density of 10^5 cells per mL into TP medium bubbled with filtered air or a mixture of 1% CO_2 and air. Growth was monitored by counting with a haemocytometer. Duplicates of Zn-replete (closed symbols) and Zn-limited (open symbols) cultures are shown and represent one of two experimental duplicates.

FIGURE 6. Supplemental Cu can restore plastocyanin abundance in Zn-limited cultures. Total soluble and particulate fractions were separated on a polyacrylamide gel and transferred as described in Figure 5. Top: Zn-replete cultures express a constant level of plastocyanin (PC) over the range of 2 to 80 μM supplemental Cu ion concentration. Bottom: Zn-limited cultures show a steady increase in PC with the increase in supplemental Cu. Lanes: 1 = 0 Cu, 2 = 2 μM Cu, 3 = 5 μM Cu, 4 = 10 μM Cu, 5 = 20 μM Cu, 6 = 40 μM Cu, 7 = 80 μM Cu. Note that at 80 μM Cu ion concentration, PC levels in Zn-limited cultures are still lower than PC levels in Zn-replete cultures growing with 2 μM supplemental Cu.

FIGURE 7. Crr1 is required for acclimation to Zn deficiency. (A) *crr1* and *CRR1* strains grown in TAP medium supplemented with 0, 1 μM, and 250 μM Zn. Cells were inoculated at 10^5 cells/mL and photographed after 3 days of growth. (B) Kautsky fluorescence rise and decay kinetics of strains growing

in Zn-replete or Zn-limiting conditions normalized to maximum fluorescence intensity measured upon exposure to a saturating light pulse (1100 µmol photons m^{-2} s^{-1}). Symbols: squares, *CRR1* in Zn-replete medium; circles, *CRR1* in Zn-limited medium; diamonds *crr1* in Zn-limited medium; and triangles, *crr1* in Zn-replete medium. (C) Cyt (solid symbols) and P_{700} (open symbols) redox changes of dark-adapted cells as measured by absorbance changes (same symbol legend as above). (D) cytochrome:P_{700} and PSI:PSII ratios. In panels A, B and C representative data are shown. For panel D, the error bars represent the s.d. of 3 independent measurements.

FIGURE 8. Zn-deficient Chlamydomonas cells accumulate other metal ions. Intracellular metal ion concentrations of Zn (A), Cu (B), Mn (C), and Fe (D) were quantified as a function of supplemental Zn. Chlamydomonas strain CC-4532 was grown in TAP medium supplemented with 0, 0.025, 0.25 (Experiment 1), 2.5 25, 80, 125, or 250 µM (Experiment 2) Zn. For analysis, cells were collected by centrifugation. The cell pellet was washed with 1 mM EDTA to remove extracellular bound metal and dissolved in 30% nitric acid by incubation at 65˚C. The metal content was measured by ICP-MS. Data points represent the average of experimental triplicates.

Table 1. Subsets of CO_2, Cu, and Zn-responsive genes are highly upregulated in Zn-limitation. Comparison of mRNA abundances among genes that are the most highly upregulated in Zn-limited relative to Zn-replete photoheterotrophic wild-type cells identifies genes known previously to be regulated by CO_2, Cu, and Zn. Protein ID Augustus 10.2 = loci identified in the Augustus update 10.2 annotation of the JGI assembly v4 for each gene. RPKM = reads per kilobase of transcript mappable length per million mapped reads. Fold change is presented as the ratio of −Zn/+Zn. Differential expression statistics are provided in terms of p-values.

Protein ID Augustus 10.2	Gene name	Defline	−Zn (RPKM)	+Zn (RPKM)	Fold change	p-value
Cre02.g118400.t1.2	*ZCP2*	expressed hypothetical protein	614	0.08	7×10^{3}	2×10^{-41}
Cre16.g651050.t1.1	*CYC6*	cytochrome c_6	1825	0.25	7×10^{3}	6×10^{-41}
Cre10.g436450.t1.1		expressed hypothetical protein	114	0.03	4×10^{3}	5×10^{-33}
Cre03.g177250.t1.1	*HAP3*	haloperoxidase-like protein	304	0.18	1×10^{3}	2×10^{-32}
Cre07.g351950.t1.2	*ZRT1*	zinc-nutrition responsive transporter	563	0.40	1×10^{3}	7×10^{-38}
Cre07.g352000.t1.1		expressed hypothetical protein	4364	4.3	1×10^{3}	1×10^{-37}
Cre13.g573950.t1.2	*ZRT3*	zinc-nutrition responsive transporter	171	0.19	1×10^{3}	2×10^{-29}

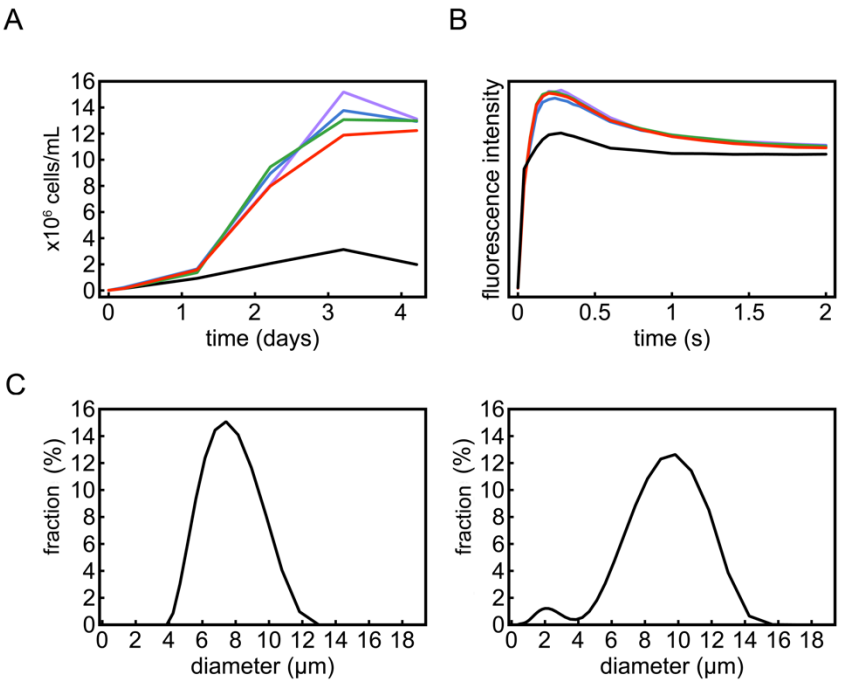

FIGURE 1. Phenotypes of Zn-deficient Chlamydomonas. Strain CC-4532 was grown in TAP medium with different amounts of supplemental Zn (in μM): 0 (black), 0.25 (blue), 2.5 (green), 80 (purple), and 250 (red). (A) Growth measured by counting cells, (B) Kautsky fluorescence rise and decay kinetics, (C) diameters of cells growing in medium containing 2.5 μM Zn (left) and 0 supplemental Zn (right). Growth curves represent the averages of biological triplicates from three separate inocula (s.d. not shown for clarity). For fluorescence measurements and cell size determination, representative data from experimental triplicates are shown.

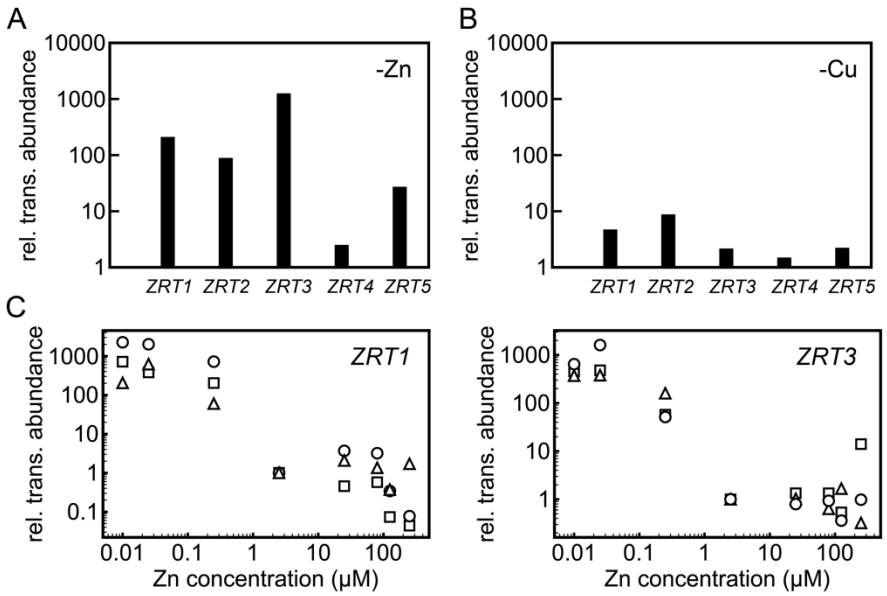

FIGURE 2. Relative expression of ZIP family transporter genes identifies a subset responsive to Zn nutrition. RNA was isolated from cells grown in TAP medium containing various amounts of Zn or Cu supplementation as described below. RNA abundance was assessed by real-time RT-PCR using the $2^{-\Delta\Delta C_T}$ method. RNA abundance was normalized to *CBLP* abundance, and average C_T values were calculated from technical triplicates. Each data point represents an independent RNA sample. (A) RNA abundance in 0 Zn relative to 2.5 μM Zn supplementation. (B) RNA abundance in 0 Cu relative to 2 μM Cu supplementation. (C) *ZRT1* (left) and *ZRT3* (right) mRNA abundances in cells grown in medium containing 0, 0.025, 0.25, 2.5, 25, 80, 125, and 250 μM supplemental Zn. The Zn deficient state was identified as the concentration of supplemental Zn at which *ZRT1* (left) and *ZRT3* (right) transcripts increased relative to 2.5 μM Zn supplementation (replete conditions).

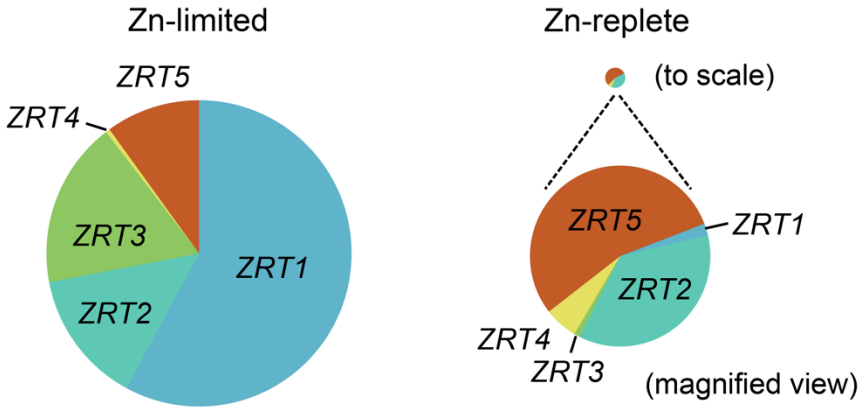

FIGURE 3. Abundance of Chlamydomonas *ZRT* transcripts. Pie charts show the contribution of each *ZRT* transcript during growth in Zn-limited (no supplemental Zn) and Zn-replete (2.5 µM Zn) media. The size of each pie chart represents the sum of all *ZRT* transcripts in that condition relative to the other.

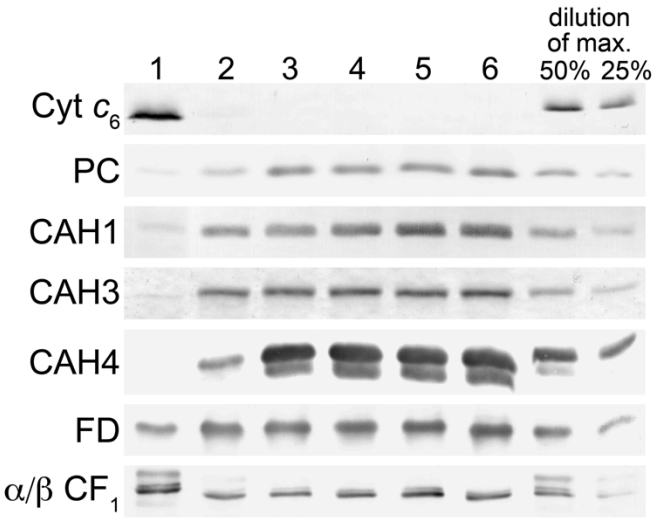

FIGURE 4. Impact of Zn nutrition on abundance of select proteins in the photosynthetic apparatus. Total soluble and resuspended particulate fractions from Chlamydomonas cultures grown in TAP medium with the various supplemental Zn concentrations were separated on polyacrylamide gels under denaturing conditions. Lanes: 1 = 0 Zn, 2 = 0.25 µM Zn, 3 = 2.5 µM Zn, 4 = 25 µM Zn, 5 = 80 µM Zn, 6 = 125 µM Zn. The separated proteins were transferred to nitrocellulose membranes. Proteins of interest were detected by immunoblot analysis with antisera raised against cytochrome c_6 (Cyt c_6), plastocyanin (PC), carbonic anhydrase 1 (CAH1), carbonic anhydrase 3 (CAH3), carbonic anhydrase 4 (CAH4), ferredoxin (FD), and the alpha and beta subunits of the chloroplast ATP synthase (α/ß CF_1). For Cyt c_6 and α/ß CF_1, dilutions of max. are based on lane 1. For all other proteins, dilutions of max. are based on lane 6.

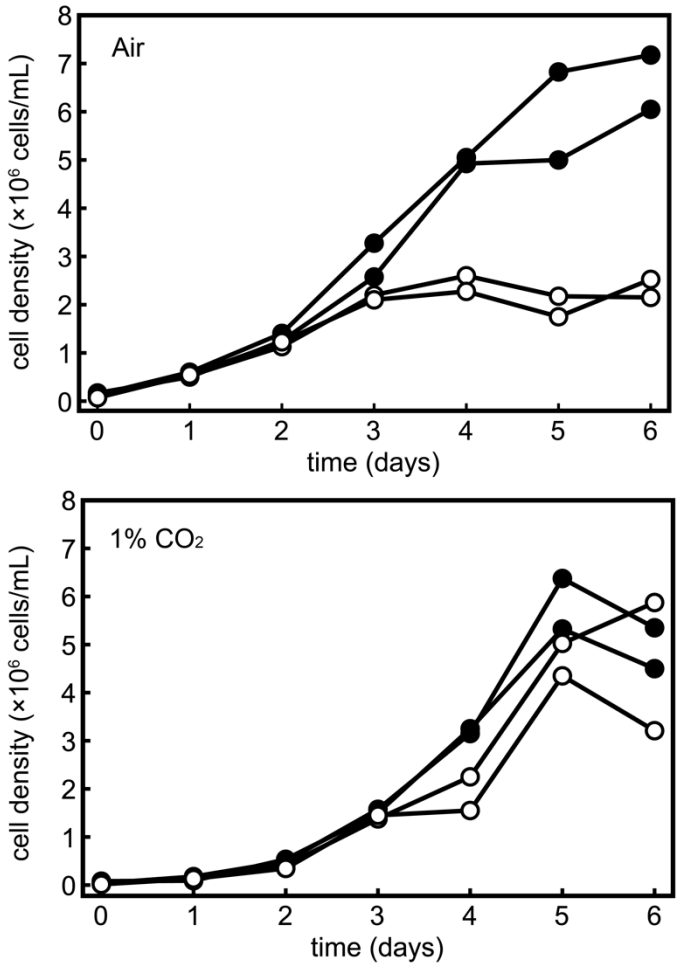

FIGURE 5. High CO_2 suppresses the growth phenotype of Zn-limited photoautotrophically grown cells. Chlamydomonas cells (strain CC-4532) were pre-conditioned in TP medium and inoculated to a density of 10^5 cells per mL into TP medium bubbled with filtered air or a mixture of 1% CO_2 and air. Growth was monitored by counting with a haemocytometer. Duplicates of Zn-replete (closed symbols) and Zn-limited (open symbols) cultures are shown and represent one of two experimental duplicates.

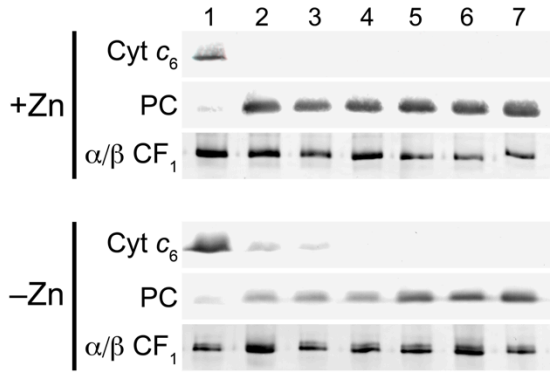

FIGURE 6. Supplemental Cu can restore plastocyanin abundance in Zn-limited cultures. Total soluble and particulate fractions were separated on a polyacrylamide gel and transferred as described in Figure 5. Top: Zn-replete cultures express a constant level of plastocyanin (PC) over the range of 2 to 80 μM supplemental Cu ion concentration. Bottom: Zn-limited cultures show a steady increase in PC with the increase in supplemental Cu. Lanes: 1 = 0 Cu, 2 = 2 μM Cu, 3 = 5 μM Cu, 4 = 10 μM Cu, 5 = 20 μM Cu, 6 = 40 μM Cu, 7 = 80 μM Cu. Note that at 80 μM Cu ion concentration, PC levels in Zn-limited cultures are still lower than PC levels in Zn-replete cultures growing with 2 μM supplemental Cu.

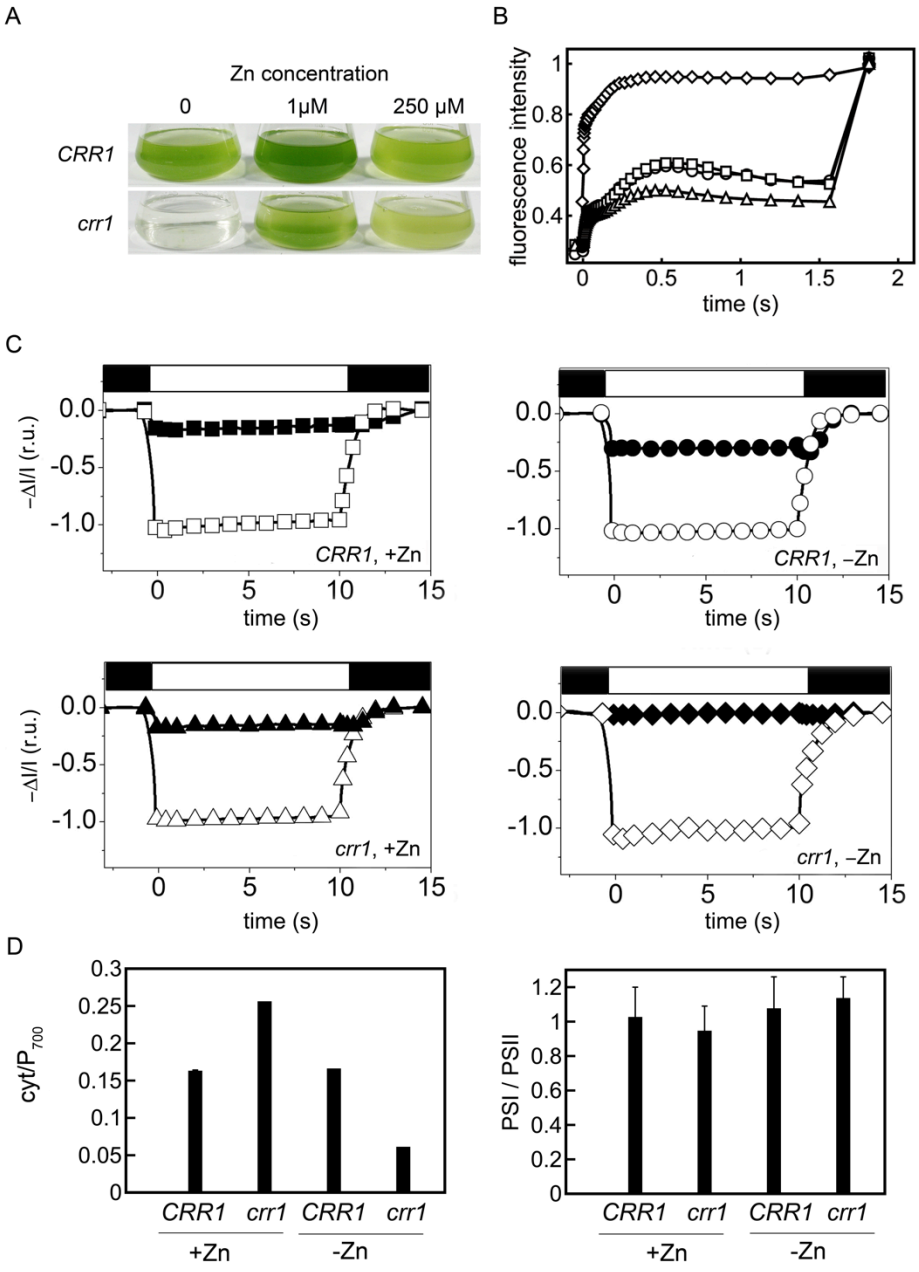

FIGURE 7. Crr1 is required for acclimation to Zn deficiency. (A) *crr1* and *CRR1* strains grown in TAP medium supplemented with 0, 1 μM, and 250 μM Zn. Cells were inoculated at 10^5 cells/mL and photographed after 3 days of growth. (B) Kautsky fluorescence rise and decay kinetics of strains growing in Zn-replete or Zn-limiting conditions normalized to maximum fluorescence intensity measured upon exposure to a saturating light pulse (1100 μmol photons m^{-2} s^{-1}). Symbols: squares, *CRR1* in Zn-replete medium; circles, *CRR1* in Zn-limited medium; diamonds *crr1* in Zn-limited medium; and triangles, *crr1* in Zn-replete medium. (C) Cyt (solid symbols) and P_{700} (open symbols) redox changes of dark-adapted cells as measured by absorbance changes (same symbol legend as above). (D) cytochrome:P_{700} and PSI:PSII ratios. In panels A, B and C representative data are shown. For panel D, the error bars represent the s.d. of 3 independent measurements.

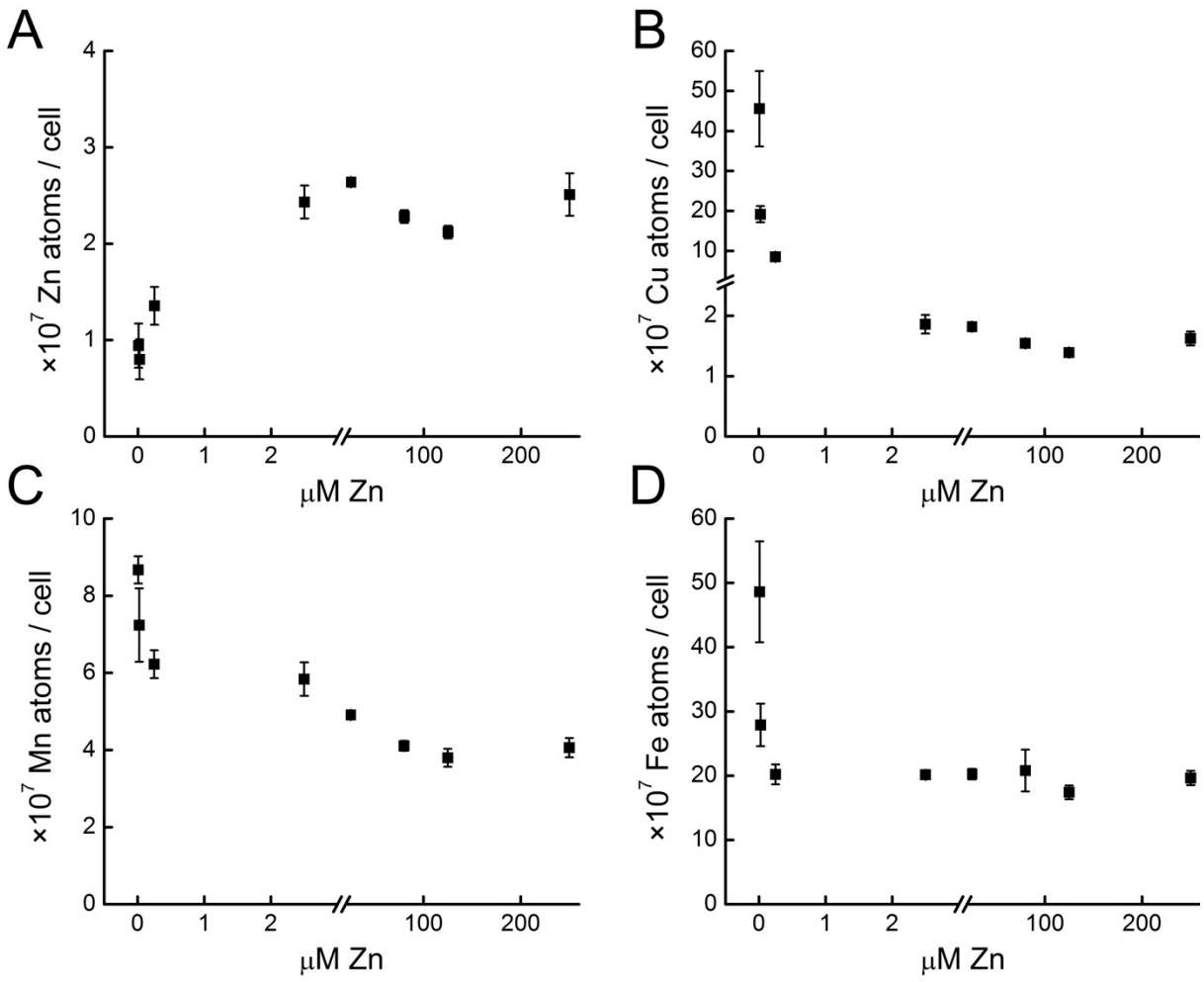

FIGURE 8. Zn-deficient Chlamydomonas cells accumulate other metal ions. Intracellular metal ion concentrations of Zn (A), Cu (B), Mn (C), and Fe (D) were quantified as a function of supplemental Zn. Chlamydomonas strain CC-4532 was grown in TAP medium supplemented with 0, 0.025 (Experiment 1), 0.25, 2.5 25, 80, 125, or 250 μM (Experiment 2) Zn. For analysis, cells were collected by centrifugation. The cell pellet was washed with 1 mM EDTA to remove extracellular bound metal and dissolved in 30% nitric acid by incubation at 65˚C. The metal content was measured by ICP-MS. Data points represent the average of experimental triplicates.